

On Symmetry Restoration at Finite Temperature (Scalar Case)

M. BORDAG*

University of Leipzig, Institute for Theoretical Physics

Augustusplatz 10/11, 04109 Leipzig, Germany

and

V. SKALOZUB†

Dnepropetrovsk State University, 320625 Dnepropetrovsk, Ukraine

March 14, 2018

Abstract

We investigate the effective potential for a scalar Φ^4 theory with spontaneous symmetry breaking at finite temperature. All 'daisy' and 'super daisy' diagrams are summed up and the properties of the corresponding gap equation are investigated. It is shown exactly that the phase transition is first order.

1 Introduction

The investigation of quantum fields at finite temperature is an important problem for modern cosmology and particle physics. Since the pioneering papers by Kirzhnits [1] and Linde [2] numerous investigations devoted to the development of the formalism and to various applications appeared. The best known papers are the famous ones by Weinberg [3] and Dolan and Jackiw [4]. There are excellent books [5, 6, 7, 8] and reviews [9, 10, 11, 12, 13, 14, 15] on these topics. However, the complete understanding of the spontaneous symmetry breaking in the early universe remains a key problem. It becomes more important as now all particles of the Standard Model (except for the Higgs) are discovered and their characteristics like masses are known. Hence, a quantitative analysis of the electroweak phase transition can be made which allows a direct comparison with

*e-mail: Michael.Bordag@itp.uni-leipzig.de

†e-mail: Skalozub@ff.dsu.dp.ua

the cosmological constraints among which the most important is the possibility of the baryogenesis scenario [15], [16]. There is a lot of papers devoted to these problems (see, for instance, [17], [18], [14] and references therein), where the temperature effects are taken into account with different accuracy. Of course, in order to make such calculations reliable, the theoretical foundations of the formalism must be deeply understood. But there are some subtle problems to solve the present paper is devoted to.

The main problem in field theory at finite temperature with symmetry breaking is the presence of long range correlations resp. infrared divergencies [9, 12, 10, 14]. To some extent, the perturbative approach itself became questionable. The point is the necessity to go beyond perturbation theory, i.e., beyond the simple expansion in powers of the coupling constant. One has to sum up certain classes of diagrams and to show that thereafter no infrared (or other) divergencies are left. There is a large number of papers trying to accomplish this task. Quite early it was understood that the so called 'daisy' diagrams must be summed up. Already in [4] it was said that even more is necessary – one has to consider the corresponding gap equation (an approximated version of the Dyson equation). However, to our knowledge, up to now no complete investigation of this kind had been done. For instance, the problem with the imaginary part of the effective action was not solved completely. Frequently, only the high temperature approximations of the corresponding quantities had been used for that investigations (see for example [19, 18]). Although the order of magnitude is captured right by this approximation, there is a reason to expect that a more correct calculation at finite (instead of high) temperature may change the results for about 10 ... 20 % which may be important in cosmological estimates. The gap equation was considered in [20] including a higher self energy graph in the gap equation. A first order transition was found, however with unwanted imaginary parts. Similar results have been found in [21].

There is another approach using flow equations based on the averaged action method ([22] and subsequent papers) where the phase transition was found to be of second order. Concerning the order of the phase transition the same result was obtained in [23] using standard renormalization group equation in $\phi_{(3)}^6$ and $\phi_{(4)}^4$ theories. However, in both approaches there is no sufficiently strong estimate for the neglected contributions.

In the present paper, in order to investigate these problems, we consider the scalar Φ^4 theory in 4(=3+1) dimensions with spontaneous symmetry breaking at finite temperature in Matsubara representation. Using functional methods we sum up all 'daisy' and 'super daisy' diagrams and all 'tadpole diagrams' as well. For the effective mass we obtain the corresponding gap equation. All important properties of its solutions are derived exactly, approximative methods and numerical calculations are given. The effective potential is shown to have a first order phase transition, all characteristic quantities are calculated, numerically where necessary. The imaginary parts of the effective mass and the effective potential

are shown to be absent in the minima of the effective potential at any temperature. So the summation made turns out to deliver the essential properties of the effective potential correctly. Further corrections may add powers in the coupling only. The methods used are in fact transparent and quite elementary, however some background in functional methods is helpful.

To the authors knowledge, this result had not been obtained before. All previous works have been done in one or other weaker approximation, frequently using high temperature expansions. We discuss the most important of these approximations in detail showing their relations to the correct values. As it frequently happens, the correct approximation is more elegant and technically simpler than the intermediate ones.

In the next section the necessary functional formalism is introduced and the summation of the infrared dangerous graphs is made. In the third section which constitutes the main part of the paper the gap equation is investigated and all important properties of its solution are derived. In the fourth section the effective potential is investigated in detail and the phase transition is shown to be of first order. In the following section the comparison with different approaches is made. The results are discussed in the conclusions and some basic functions used are collected in the appendix.

2 Perturbative field theory in functional formulation

The appropriate formulation of perturbative quantum field theory is the functional formulation. We follow the book [24] which gives the most complete treatment of this formalism. Similar representations are given in [7] and in [25].

Let us first consider a general Euclidean scalar theory with the action

$$S(\Phi) = \frac{1}{2}\Phi K\Phi - \frac{\gamma}{3}\Phi^3 - \frac{\lambda}{4}\Phi^4. \quad (1)$$

We use condensed notations. The arguments of all quantities like the field Φ are dropped. Wherever arguments appear they are integrated over. The first term in the action is the 'free part', quadratic in Φ . Its kernel is the operation K . In our case it is

$$K = \square - m^2. \quad (2)$$

In complete notation the action reads

$$S(\Phi) = \int dx \left(\frac{1}{2}\Phi(x)(\square - m^2)\Phi(x) - \frac{\gamma}{3}\Phi(x)^3 - \frac{\lambda}{4}\Phi(x)^4 \right). \quad (3)$$

The generating functional of the Green functions is given by

$$Z(J) = N \int D\Phi \exp \left(\frac{1}{2}\Phi K\Phi - \frac{\gamma}{3}\Phi^3 - \frac{\lambda}{4}\Phi^4 + \Phi J \right), \quad (4)$$

where N is a normalization constant and J ($J(x)$) is a source. We consider it as a functional argument. The perturbative representation of $Z(J)$ is

$$Z(J) = N \exp \left[\frac{1}{2} \frac{\delta}{\delta \Phi} \Delta \frac{\delta}{\delta \Phi} \right] \exp \left[-\frac{\gamma}{3} \Phi^3 - \frac{\lambda}{4} \Phi^4 + \Phi J \right]_{|\Phi=0}, \quad (5)$$

where $\frac{\delta}{\delta \Phi}$ denotes the variational derivative. By expanding the exponentials the last formula turns into the representation as the sum over all graphs with lines $\Delta = -K^{-1}$ and generating vertices $-\frac{\gamma}{3} \Phi^3 - \frac{\lambda}{4} \Phi^4 + \Phi J$. An actual vertex factor is the corresponding functional derivative of the generating vertex. A line is 'hung up' by the variational derivatives between two (or one and the same) vertices.

The generating functional of the connected Green functions is known to be

$$W(J) = \ln Z(J). \quad (6)$$

To pass to the effective action $\Gamma(\Phi)$ one has to perform the Legendre transformation. For this reason one introduces the new functional argument $\Phi = \frac{\delta}{\delta J} W(J)$, expresses J in terms of Φ and defines the effective action by

$$\Gamma(\Phi) = W(J) - J\Phi. \quad (7)$$

Its perturbative expansion is known to be

$$\Gamma(\Phi) = S(\Phi) + \frac{1}{2} \text{Tr} \ln \Delta + W^{1\text{PI}}(J \rightarrow \Delta^{-1}\Phi). \quad (8)$$

Here, S is the action (1), the 'Tr ln' is the one loop contribution and $W^{1\text{PI}}$ denotes the one particle irreducible (1PI) graphs contributing to W , by means of $J \rightarrow \Delta^{-1}\Phi$ amputated for their external legs.

Now the effective potential is minus the effective action for zero argument¹:

$$V_{\text{eff}} = -\Gamma(0). \quad (9)$$

In the graphical representation it contains the tree contribution $S(0)$ (which is zero for the action (1)), the 'Tr ln' as the one loop contribution and $W^{1\text{PI}}(0)$, the 1PI vacuum graphs of W .

In general, in the representation by graphs, lines closed over one vertex, , do appear. In field theory without external fields or without symmetry breaking resp. at $T = 0$ these result in unessential constants and are usually hidden in a normalization. However, for finite temperature they deliver nontrivial contributions and must be taken seriously. In fact, from the considered Φ^4 -vertex they appear with two external legs, . These insertions are called *daisy* graphs.

¹Usually this notation is preserved for a constant background field. Up to now the formulas are completely general and the background is not specified.

They are like mass insertions. As such they cause the known infrared problems. Consequently, they must (and, in fact, can) be summed up completely. The same holds for *tadpole* insertions,  , appearing from Φ^3 -vertices.

The problem of summation had been tackled repeatedly. Difficulties arise with respect to the correct count of the symmetry coefficients and beside. Here we use a simple functional method to sum up these insertions completely. From the point of view of the functional methods as described in the book [24] this is an easy exercise consisting in adding and subtracting three terms in the action, i.e., in redistributing contributions between the 'free part' and the remaining part, which is treated perturbatively. So we rewrite the action S (1) in the form

$$S = \frac{1}{2} \Phi \left(\square - m^2 - a^2 \right) \Phi - b^2 - c\Phi + \mathcal{M}_4 + \mathcal{M}_3, \quad (10)$$

where the new vertex factors $\mathcal{M}_4 \equiv \frac{\lambda}{4}\Phi^4 + \frac{1}{2}a^2\Phi^2 + b^2$ and $\mathcal{M}_3 \equiv \frac{\gamma}{3}\Phi^3 + c\Phi$ are introduced. For the moment the parameters a , b and c are arbitrary constants.

In the functional language all lines closed over one vertex result from the operation of 'hanging up lines' acting only on that vertex. So, for instance, the daisies on one Φ^4 -vertex are generated by

$$\exp \left[\frac{1}{2} \frac{\delta}{\delta \Phi} \Delta \frac{\delta}{\delta \Phi} \right] \Phi^4 = \Phi^4 + 6\Delta_0 \Phi^2 + 3\Delta_0^2, \quad (11)$$

where Δ_0 is Δ for coinciding arguments (see (12)). A detailed explanation can be found in [24]. Nevertheless, these formulae call for a more detailed explanation here. First of all, the line Δ has two ends and, hence, it is the function of two arguments. For example, in free space it is nothing else than the propagator $\Delta(x, y) = \int \frac{dk}{(2\pi)^4} \frac{\exp(ik(x-y))}{k^2 + m^2}$. The operation with the functional derivatives reads

$$\frac{1}{2} \frac{\delta}{\delta \Phi} \Delta \frac{\delta}{\delta \Phi} = \frac{1}{2} \int dx \int dy \frac{\delta}{\delta \Phi(x)} \Delta(x, y) \frac{\delta}{\delta \Phi(y)}.$$

The vertex is $\Phi^4 = \int dx \Phi(x)^4$ and the closed line is represented by

$$\Delta_0 = \Delta(x, y)|_{x=y} = \int \frac{dk}{(2\pi)^4} \frac{1}{k^2 + m^2} \quad (12)$$

(for the moment we ignore the convergence problems). The index '0' is used to symbolize that the line $\Delta(x, y)$ is taken at $x - y = 0$. Now, in the explicit notations, the derivatives can be carried out trivially and returning back to the condensed notations the rhs. of Eq. (11) will be obtained. Analogously, the relation

$$\exp \left[\frac{1}{2} \frac{\delta}{\delta \Phi} \Delta \frac{\delta}{\delta \Phi} \right] \Phi^3 = \Phi^3 + 3\Delta_0 \Phi \quad (13)$$

can be checked. It describes the emergence of the tadpole diagrams from a Φ^3 -vertex.

In order to avoid the appearance of 'daisies' the constants a and b introduced in Eq. (10) may be adjusted accordingly. In demanding

$$\exp \left[\frac{1}{2} \frac{\delta}{\delta \Phi} \tilde{\Delta} \frac{\delta}{\delta \Phi} \right] \mathcal{M}_4 = -\frac{\lambda}{4} \Phi^4 \quad (14)$$

this goal can be achieved. At this point it must be noted that by 'adding zero' in Eq. (10) we changed the first part of the action which is the 'free part' giving rise to the lines (compare Eqs. (4) and (5)). Hence the mass in the propagator is changed according to $m^2 \rightarrow m^2 + a^2$. We denote the line with this changed mass by a tilde.

From the formula (11) together with the simpler one

$$\exp \left[\frac{1}{2} \frac{\delta}{\delta \Phi} \Delta \frac{\delta}{\delta \Phi} \right] \Phi^2 = \Phi^2 + \Delta_0, \quad (15)$$

we obtain

$$\begin{aligned} \exp \left[\frac{1}{2} \frac{\delta}{\delta \Phi} \tilde{\Delta} \frac{\delta}{\delta \Phi} \right] \exp(\mathcal{M}_4) &\equiv \exp \left[\frac{1}{2} \frac{\delta}{\delta \Phi} \tilde{\Delta} \frac{\delta}{\delta \Phi} \right] \left(-\frac{\lambda}{4} \Phi^4 + \frac{a^2}{2} \Phi^2 + b^2 \right) \\ &= -\frac{\lambda}{4} \Phi^4 + \left(-\frac{3}{2} \lambda \tilde{\Delta}_0 + \frac{a^2}{2} \right) \Phi^2 - \frac{3}{4} \lambda \tilde{\Delta}_0^2 + \frac{a^2}{2} \tilde{\Delta}_0 + b^2. \end{aligned}$$

In order to fulfill the requirement (14) the equations

$$a^2 = 3\lambda \tilde{\Delta}_0 \quad (16)$$

and

$$b^2 = -\frac{3}{4} \lambda \tilde{\Delta}_0^2 \quad (17)$$

must be satisfied.

In a similar way we obtain from (13)

$$\begin{aligned} \exp \left[\frac{1}{2} \frac{\delta}{\delta \Phi} \tilde{\Delta} \frac{\delta}{\delta \Phi} \right] \exp(\mathcal{M}_3) &\equiv \exp \left[\frac{1}{2} \frac{\tilde{\delta}}{\delta \Phi} \Delta \frac{\delta}{\delta \Phi} \right] \left(-\frac{\gamma}{3} \Phi^3 + c \Phi \right) \\ &= -\frac{\gamma}{3} \Phi^3 + \left(-\frac{3}{2} \gamma \tilde{\Delta}_0 + c \right) \Phi \end{aligned}$$

and from the requirement

$$\exp \left[\frac{1}{2} \frac{\delta}{\delta \Phi} \tilde{\Delta} \frac{\delta}{\delta \Phi} \right] \mathcal{M}_3 = -\frac{\gamma}{3} \Phi^3 \quad (18)$$

the parameter c follows to be

$$c = \frac{3}{2} \gamma \tilde{\Delta}_0. \quad (19)$$

So, by virtue of (14) and (18), no closed lines will appear from the vertices \mathcal{M}_3 and \mathcal{M}_4 . This is a quite strong consequence because together with the 'daisy'

diagrams also all 'super daisy'² diagrams appear to be summed up. The same holds for the 'tadpole' diagrams. This procedure is similar to the concept of the 'reduced vertex' in [24], p. 38.

The meaning of Eq. (16) is well known - it is a special case of the Dyson equation, also called 'gap equation'. We shall follow the latter terminology. To illustrate this we denote the mass of the line as explicit argument of the function $\tilde{\Delta}_0$ as $\tilde{\Delta}_0(M)$, where $M^2 = m^2 + a^2$. In this notation the Δ without tilde is $\Delta_0(m)$. So we drop the 'tilde' in what follows. Than Eq. (16) becomes

$$M^2 = m^2 + 3\lambda\Delta_0(M). \quad (20)$$

M has the meaning of the *effective mass*.

We note the graphical representation of $\Delta_0(M)$,

$$-3\lambda\Delta_0(M) = \text{---} = -3\lambda \int \frac{dk}{(2\pi)^4} \frac{1}{k^2 + M^2}. \quad (21)$$

Now we turn to the corresponding theory with temperature using the Matsubara formalism. Thereby the formulae given above remain unchanged. Further we introduce the spontaneous symmetry breaking by giving the mass term the 'wrong sign'. Than, after $m^2 \rightarrow -m^2$ the field Φ must be shifted

$$\Phi(x) = \Phi_c + \eta(x), \quad (22)$$

in order to quantize in the vicinity of the lower lying minimum of the action, where Φ_c is the condensate field, a constant, and $\eta(x)$ is to be quantized. After this substitution the action reads

$$S = \frac{m^2}{2}\Phi_c^2 - \frac{\lambda}{4}\Phi_c^4 + \Phi_c(m^2 - \lambda\Phi_c^2)\eta + \frac{1}{2}\eta(\square - \mu^2)\eta - \lambda\Phi_c\eta^3 - \frac{\lambda}{4}\eta^4, \quad (23)$$

where $\mu^2 = -m^2 + 3\lambda\Phi_c^2$ is the new mass parameter squared. Using this action instead of (1) and performing the summation of the 'daisy' graphs as explained just above the action takes the form

$$\begin{aligned} S(\eta) = & \frac{m^2}{2}\Phi_c^2 - \frac{\lambda}{4}\Phi_c^4 + \frac{3}{4}\lambda\Delta_0(M)^2 + \Phi_c(-m^2 + \lambda\Phi_c^2 + 3\lambda\Delta_0(M))\eta \\ & + \frac{1}{2}\eta(\square - M^2)\eta - \lambda\Phi_c\mathcal{M}_3 - \frac{\lambda}{4}\mathcal{M}_4, \end{aligned} \quad (24)$$

where

$$\mathcal{M}_3 = \eta^3 + 3\lambda\Delta_0(M)\eta \quad (25)$$

and

$$\mathcal{M}_4 = \eta^4 + 6\lambda\Delta_0(M)\eta^3 - \frac{3}{4}\lambda\Delta_0(M)^2 \quad (26)$$

²They are also called 'foam' diagrams in [26].

are the vertices which do not obtain closed loops over themselves in the perturbative expansion assuming the equation (20) holds which reads

$$M^2 = -m^2 + 3\lambda\Phi_c^2 + 3\lambda\Delta_0(M) \quad (27)$$

in the present notations.

According to the general formula (8), the effective action takes now the form

$$\begin{aligned} \Gamma(\eta) = & -V_{\text{eff}} + \Phi_c \left(-m^2 + \lambda\Phi_c^2 + 3\lambda\Delta_0(M) \right) \eta + \frac{1}{2}\eta \left(\square - M^2 \right) \eta \\ & -\lambda\Phi_c\mathcal{M}_3 - \frac{\lambda}{4}\mathcal{M}_4 + \tilde{W}^{\text{1PI}}(\eta), \end{aligned} \quad (28)$$

where

$$V_{\text{eff}} = -\frac{m^2}{2}\Phi_c^2 + \frac{\lambda}{4}\Phi_c^4 - \frac{3}{4}\lambda\Delta_0^2(M) + V_1(M) - W^{\text{1PI}}(0) \quad (29)$$

is the effective potential and

$$V_1 = -\frac{1}{2} \text{Tr} \ln \Delta$$

is the one loop contribution with the mass M in the propagator, see Eq. (53).

In the effective action $\Gamma(\eta)$, (28), as well as in the action (24), the term linear in η acquired an additional contribution. The effective mass M in the addendum quadratic in η must obey the gap equation (27) and becomes a function of the condensate Φ_c and of the temperature in this way: $M(\Phi_c; \lambda, T)$. All higher graphs with external legs are contained in \tilde{W}^{1PI} .

In the effective potential V_{eff} the first two terms are the so called 'tree' approximation. The corresponding minimum of the effective potential is reached at $\Phi_c = m/\sqrt{\lambda}$ which is at once the condition for the linear term in Γ to vanish at tree level and the mass of the field is $M^2 = 2m^2$, then.

The third term in V_{eff} can be represented graphically as  looking like a 'eight'. The function V_1 is a notation for the 'Tr ln' contribution and $W^{\text{1PI}}(0)$ are the higher loop graphs without external legs (vacuum graphs). We do not need to consider them in this paper.

The effective potential has to be considered together with the gap equation (27). This allows to exclude $\Delta_0(M)$ from explicitly appearing in the expression

$$V_{\text{eff}} = -\frac{(M^2 + m^2)^2}{12\lambda} + \frac{M^2}{2}\Phi_c^2 - \frac{\lambda}{2}\Phi_c^4 + V_1(M), \quad (30)$$

which, together with (27), will be used in the following.

The functions $\Delta_0(M)$ and $V_1(M)$ can be written down quite explicitly. This had been done in a number of papers. Different representations are possible. We collect the two most useful ones in the Appendix together with their expansions

for high T which is at once the expansion for small M . These quantities contain ultraviolet divergencies which are removed by a standard procedure which includes also the fixing of the normalization conditions. They are chosen not to change the minimum of the effective potential known at tree level in case of zero temperature (the finite temperature contributions are ultraviolet finite and unique). So we require

$$\frac{\partial V_1}{\partial \Phi_c|_{\Phi_c=m/\sqrt{\lambda}}} = 0 \quad \text{and} \quad \frac{\partial^2 V_1}{\partial \Phi_c^2|_{\Phi_c=m/\sqrt{\lambda}}} = 0.$$

In fact, the superficial divergence degree of vacuum graphs is four. Because V_{eff} depends on Φ_c^2 rather than on Φ_c , there are only three independent normalization conditions to impose. After the first two there remains one condition fixating the value of V_{eff} at some value of Φ_c^2 . It is natural to demand $V_{\text{eff}}(\Phi_c = 0) = 0$. But the calculation of the corresponding constant to be subtracted from V_{eff} is not easy. So we leave that condition open. In fact, it becomes important only in figure 4 where it had been adjusted numerically.

The single 'daisy' graph Δ_0 , which is in fact the first graph in the self energy, has superficial degree two and two normalization conditions have to be imposed. In the same aim as above we choose

$$\Delta(M^2)|_{\Phi_c=m/\sqrt{\lambda}} = 0.$$

The second condition results in an additive constant. We choose it so that the equation

$$\frac{1}{M} \frac{\partial V_1(M)}{\partial M} = \Delta_0(M) \tag{31}$$

holds. Note that this relation holds for the temperature dependent part automatically.

3 Solving the Gap Equation

The solution of the gap equation is the key element of the whole procedure. There is, of course, no explicit solution. However, the most important properties can be derived exactly.

In solving the gap equation (27) we obtain the effective mass M appearing after summing up the 'daisy' diagrams. It is a function of the condensate Φ_c , further it depends on the bare mass m , on the coupling λ and on the temperature T : $M(\Phi_c; m, \lambda, T)$. The inverse function, $\Phi_c(M; m, \lambda, T)$ is given explicitly by Eq. (27): $\Phi_c^2 = (M^2 + m^2 - 3\lambda\Delta(M))/3\lambda$. This function can be easily plotted, see Figure 1, for real values of M . As seen, it is not monotone and the inverse function, i.e., $M(\Phi_c; m, \lambda, T)$ is not unique. So the gap equation has two solutions in M for each Φ_c . In order to understand that better we consider the graphic

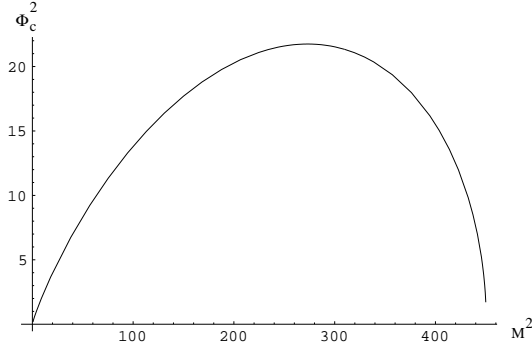


Figure 1: The function $\Phi_c^2(M^2)$ as given by the gap equation (27) for $\lambda = 5$ and $T = 1$

solution of Eq. (27). For this we write the equation in the form $M^2 = r_{hs}(M)$ with the notation $r_{hs}(M) = -m^2 + 3\lambda\Phi_c^2 + 3\lambda\Delta_0(M)$ and plot the lhs. and the rhs. of this equation as functions of M^2 in one picture, see figure 2. The curve for the rhs. starts at $M = 0$ in $r_{hs}|_{M=0} = -m^2\delta_1 + 3\lambda\Phi_c^2 + \lambda T^2/4$ which follows from (61) where we introduced the notation

$$\delta_1 = 1 - \frac{3\lambda}{8\pi^2}. \quad (32)$$

The derivative is negative there (see the second term in the rhs. of Eq. (61)) so that for $-m^2\delta_1 + 3\lambda\Phi_c^2 + \lambda T^2/4 > 0$ there is a solution close to $M = 0$. In the opposite case there is no real solution there. For large values of M , the curve describing the rhs. will be dominated by the logarithm, see formula (58). For $3\lambda \ln(M^2/2m^2)/16\pi^2 \approx 1$ it becomes larger than the lhs. and delivers the other solution, seen in Figure 1 as the decreasing part of the curve. It takes place for large values of λ and M (at any T) and is of no relevance for physical applications.

For $-m^2\delta_1 + 3\lambda\Phi_c^2 + \lambda T^2/4 = 0$ the curve of the rhs. starts in the origin and the solution is exactly $M = 0$.

In general, the solution of the gap equation is non perturbative and can be obtained only numerically. However, for the parameters in some range there are two possibilities for approximative procedures.

3.1 The Iterative Solution of the Gap Equation

Equation (27) can be iterated. For this we write it in the form $M = \sqrt{r_{hs}(M)}$. Inserting some zeroth approximation M^0 into the rhs. the next approximation $M^{(1)}$ can be obtained which in turn must be inserted into the rhs. and so on. This procedure converges until the module of the derivative of the rhs. with respect to M does not exceed unity. This derivative takes its largest value at $M = 0$. From this a sufficient criterion for the convergence can be derived. Let us consider the

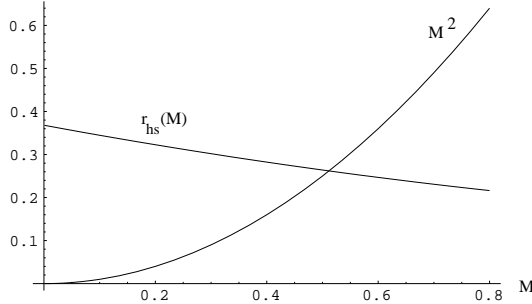


Figure 2: Plot of the rhs. and the lhs. of the gap equation (27) for $\Phi_c = 0.6$, $\lambda = 1$, $T = 1$

derivative

$$\frac{\partial r_{hs}}{\partial M} \Big|_{M=0} = \frac{-3\lambda T/4\pi}{2\sqrt{-m^2\delta_1 + 3\lambda\Phi_c^2 + \lambda T^2/4}}.$$

It is smaller than unit for

$$\lambda < \frac{4m^2}{3T^2} + \frac{32\pi^2\Phi_c^2}{3T^2} + \frac{8\pi^2}{9} + \sqrt{\left(\frac{4m^2}{3T^2} + \frac{32\pi^2\Phi_c^2}{3T^2} + \frac{8\pi^2}{9}\right)^2 - \frac{m^2}{T^2}}.$$

Also, even for λ obeying this restriction, the denominator may become small and make the iteration procedure diverge. In fact, this happens for M close to zero.

In case the sufficient conditions are satisfied the iteration procedure works well. It does so even in the complex region, i.e., for $M^2 < 0$ and down to $T \gtrsim 0$. The solution appears in powers of $\sqrt{\lambda}$.

3.2 The Approximative Solution

Instead of iterating the Eq. (27) one may approximate it and solve the approximated equation. We restrict ourselves to temperatures of order $T \gtrsim \lambda^{-\frac{1}{2}}$. This is just the order where the phase transition happens (see below). Then in the gap equation the approximation (61) may be used. So the approximated gap equation reads

$$M^2 = -m^2 + 3\lambda\Phi_c^2 + 3\lambda \left\{ \frac{T^2}{12} - \frac{MT}{4\pi} + \frac{1}{16\pi^2} \left[M^2 \left(\ln \frac{(4\pi T)^2}{2m^2} - 2\gamma \right) + 2m^2 \right] \right\}. \quad (33)$$

With the notation $\delta_2 = 1 - \frac{3\lambda}{8\pi^2} \left[\ln \frac{(4\pi T)^2}{2m^2} - 2\gamma \right]$ the solution reads

$$M = -\frac{3\lambda T}{8\pi\delta_2} + \delta_2^{-\frac{1}{2}} \sqrt{\left(\frac{3\lambda T}{8\pi\sqrt{\delta_2}}\right)^2 - m^2\delta_1 + 3\lambda\Phi_c^2 + \frac{\lambda T^2}{4}}. \quad (34)$$

Again, it can be seen that it is real for $T^2 \geq \left(\frac{4m^2}{\lambda}\delta_1 - 12\Phi_c^2\right) / \left(1 + \frac{9\lambda}{2\pi\delta_2}\right)$. Thereby, for $T^2 < \frac{4m^2}{\lambda}\delta_1$ this is the case for $\Phi_c^2 > \frac{1}{12}(\frac{4m^2}{\lambda} - T^2)$ whereas for $T^2 > \frac{4m^2}{\lambda}\delta_1$ the solution is real for any Φ_c . For $-m^2\delta_1 + 3\lambda\Phi_c^2 + \lambda T^2/4 < 0$ the solution becomes complex and the mass squared becomes negative. The solution $M^2(\Phi_c^2)$ of the gap equation is shown in figure 3 for a temperature where it has an imaginary part for small Φ_c and is real for larger Φ_c . It is a nearly linear function and follows mostly the tree solution, $M = \mu$, $\mu^2 = -m^2 + 3\lambda\Phi_c^2$. Only near $M = 0$ it shows a nontrivial behavior which is the non perturbative region discussed above.

The validity of the approximation leading to Eq. (33) can be established as follows. First, consider large T . The solution is $M = \sqrt{\lambda}T/2(1 + O(\sqrt{\lambda}))$. Second, consider $T \sim 1/\sqrt{\lambda}$. The solution is $M \lesssim \sqrt{\lambda}T$. So in both cases the contributions neglected in (61) are of order $\frac{M}{T} \sim \sqrt{\lambda}$ or smaller (for example, at $-m^2\delta_1 + 3\lambda\Phi_c^2 + \lambda T^2/4 = 0$ the solution $M = 0$ is exact). Hence including higher order terms into (61) would result in corrections of order $\sqrt{\lambda}$. On the other hand side dropping any of the terms in (61) changes the solution quantitatively. It can be checked that in doing so even the order of the phase transition changes.

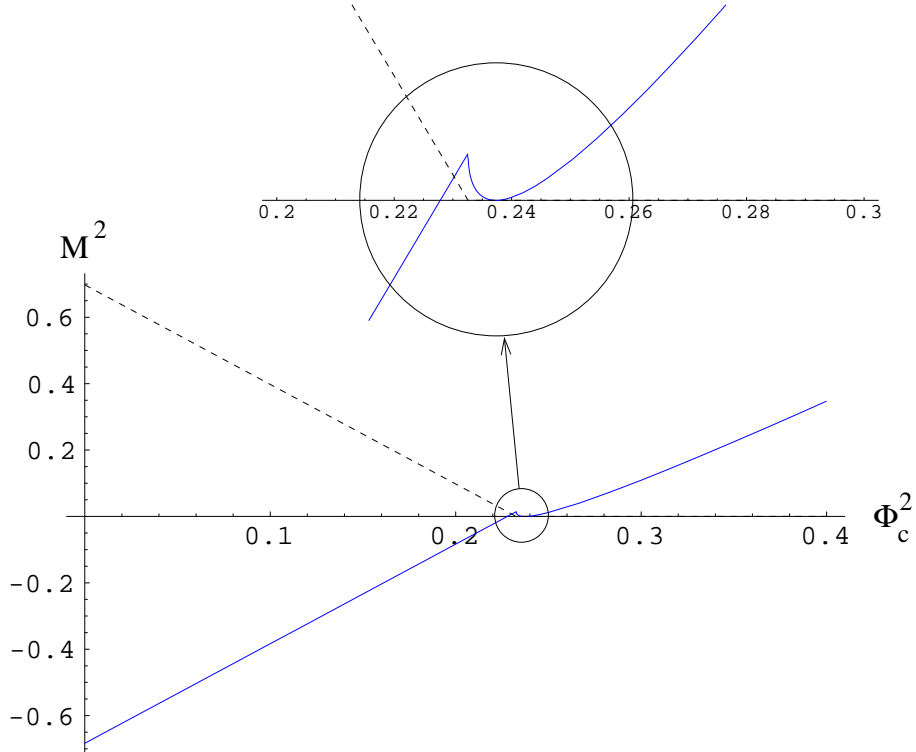


Figure 3: Real part (solid line) and imaginary part (broken line) of the effective mass squared M^2 as function of Φ_c^2 solving the gap equation for $\lambda = T = 1$, the magnification shows details near $M = 0$

4 The Shape of the Effective Potential and its Extrema

The effective mass and the effective potential can be calculated numerically and plotted. In the temperature region where the phase transition takes place the approximative solution (34) of the gap equation together with formula (57) makes it very easy to plot the effective potential as a function of Φ_c , see figure 4. It shows the typical behavior of a first order phase transition. This important property can be shown exactly.

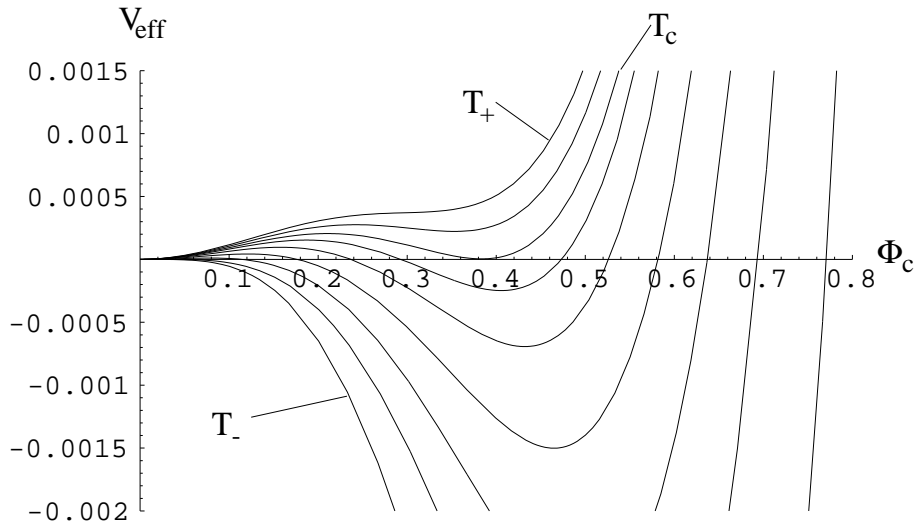


Figure 4: The effective potential as function of Φ_c for several temperatures in the region $T_- < T < T_+$ for $\lambda = 1$

We investigate the extrema of the effective potential. Differentiating V_{eff} as given by Eq. (30) we obtain

$$\frac{\partial V_{\text{eff}}}{\partial \Phi_c^2} = \left(-\frac{M^2 + m^2}{6\lambda} + \frac{1}{2}\Phi_c^2 + \frac{1}{2}\Delta_0(M) \right) \frac{\partial M^2}{\partial \Phi_c^2} + \frac{1}{2}M^2 - \lambda\Phi_c^2, \quad (35)$$

where (31) was used. By means of the gap equation (27) this expression simplifies and from the condition $\partial V_{\text{eff}} / \partial \Phi_c^2 = 0$ we obtain

$$\lambda\Phi_c^2 = \frac{M^2}{2}. \quad (36)$$

This relation must be considered together with the gap equation where we eliminate $\lambda\Phi_c^2$ by means of Eq. (27) and obtain

$$M^2 = 2m^2 - 6\lambda\Delta_0(M) \quad (37)$$

as the gap equation in the extrema of the effective potential.

Eq. (37) has a form similar to the gap equation (27). Again, we consider the graphical solution written in the form $M = \sqrt{2m^2 - 6\lambda\Delta_0(M)}$. Typical pictures are shown in figure 5.

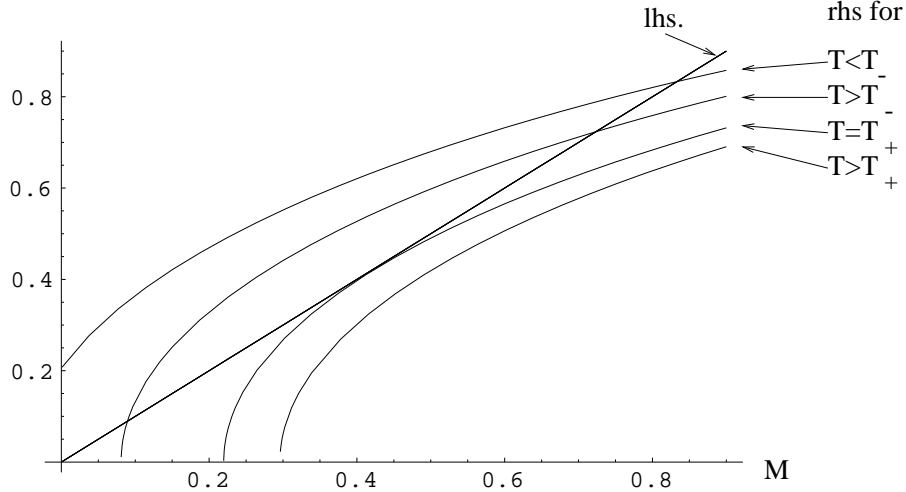


Figure 5: Plot of the rhs. and of the lhs. ($= M$) of the gap equation in the minimum as function of M for $\lambda = 1$ and several temperatures

The curve for the rhs starts in $2m^2\delta_1 - \lambda T^2/2$ with a positive derivative (cf. Eq. (61)). Therefore, for sufficiently small T there is one real solution. This is the position of a minimum of the effective potential (for $T = 0$ one obtains the known picture of the tree approximation). For $T^2 \geq 4m^2\delta_1/\lambda$ the starting point of the curve representing the rhs. is below the origin and there are two real solutions. Because the effective potential is a continuous function, this second solution must be a maximum. It appears at smaller values of Φ_c than the minimum. So

$$T_- = \frac{2m}{\sqrt{\lambda}}\sqrt{\delta_1} \quad (38)$$

is the lower spinodal temperature. Raising the temperature lowers the curve representing the rhs. further. The two solutions become closer to each other until they merge finally. At that temperature the minimum and the maximum are at the same place. Hence this is the upper spinodal temperature T_+ . For even higher temperature there is no real solution and the effective potential is a monotone function – the symmetry is restored.

Because these are exact, non perturbative properties of Eq. (37) it is shown exactly that the phase transition is of first order.

It is important to note that the effective action is real in both its minima. For $T < T_-$ there is only one minimum (that at finite Φ_c). There the effective

potential is real. This is clear because the effective mass is real as shown just above and because the functions $\Delta_0(M)$ and $V_1(M)$ are real for real arguments. In $\Phi_c = 0$ the effective potential has a maximum and it has an imaginary part. This corresponds to the instability of this state.

Consider $T_- < T < T_+$. Here the effective potential has two minima, one in $\Phi_c = 0$ and the other one at finite Φ_c . In both minima (as, in general, for any $T > T_-$) the effective potential is real. So in the given approximation they are both stable. In fact, the effective potential should have an imaginary part in the minimum at $\Phi_c = 0$ for $T < T_c$ because there is a finite probability for a tunneling transition to the lower lying minimum. But this is beyond the given approximation.

It is interesting to note that in $T = T_-$ the effective mass at $\Phi_c = 0$ vanishes. Also the second derivative is zero there, see Eq. (44). So this point is metastable as it must be in a first order phase transition.

These features can be seen explicitly in the expansion of Eq. (37) for small λ . Using (61) in the rhs. of Eq. (37) we obtain

$$M^2 = 2m^2 - 6\lambda \left\{ \frac{T^2}{12} - \frac{MT}{4\pi} + \frac{1}{16\pi^2} \left[M^2 \left(\ln \frac{(4\pi T)^2}{2m^2} \right) + 2m^2 \right] \right\}, \quad (39)$$

which can be easily resolved with respect to M . With the notations for δ_1 introduced in the preceding section and $\delta_3 = 1 + \frac{3\lambda}{8\pi^2} \left(\ln \frac{(4\pi T)^2}{2m^2} - 2\gamma \right)$ we obtain

$$M_{\text{Min/Max}} = \frac{3\lambda T}{4\pi\delta_3} \pm \sqrt{\left(\frac{3\lambda T}{4\pi\delta_3} \right)^2 + \frac{2m^2\delta_1}{\delta_3} - \frac{\lambda T^2}{2\delta_3}}, \quad (40)$$

where the upper sign corresponds to the minimum and the lower sign to the maximum of the effective potential. The condensate Φ_c is related to this mass by Eq. (36). The lower spinodal temperature T_- is the temperature at which the maximum appears at $M_{\text{Max}} = 0$ when raising the temperature. It is the same as given by formula (38). Also, the upper spinodal temperature T_+ follows from formula (39). It is the temperature for which the positions of the maximum and of the minimum coincide, i.e., where the square root vanishes:

$$T_+ = \frac{2m}{\sqrt{\lambda}} \sqrt{\frac{\delta_1}{1 - \frac{9\lambda}{8\pi^2\delta_3}}}. \quad (41)$$

Within the given precision³, i.e., in the lowest nontrivial order in λ , these temperatures can be written as

$$T_- = \frac{2m}{\sqrt{\lambda}} \left(1 - \frac{3\lambda}{16\pi^2} \right), \quad T_+ = \frac{2m}{\sqrt{\lambda}} \left(1 + 2\frac{3\lambda}{16\pi^2} \right). \quad (42)$$

³bearing in mind that corrections of order λ^2 and higher follow from the graphs contained in $W^{1\text{PI}}(0)$, Eq. (29)

They are both of order $m/\sqrt{\lambda}$ justifying the approximation made in the gap equation. The interval between T_- and T_+ is of order $\sqrt{\lambda}m$.

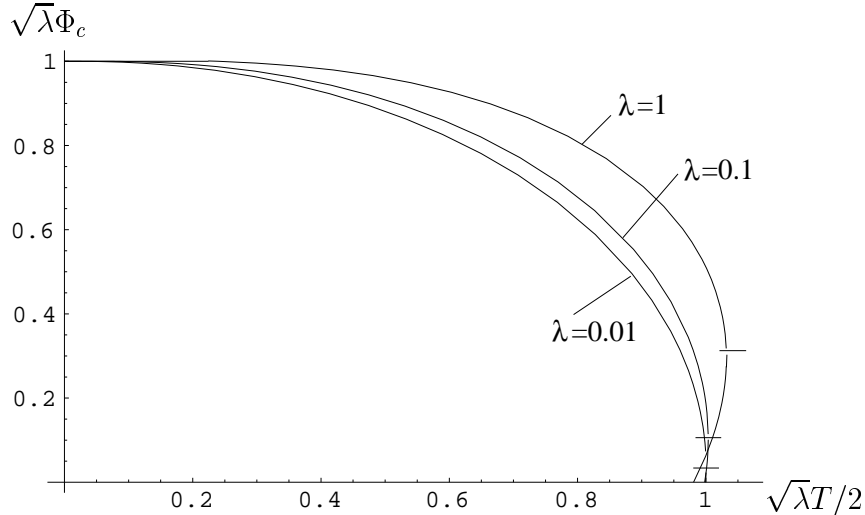


Figure 6: $\sqrt{\lambda}\Phi_c = M/\sqrt{2}$ in the minimum (resp. maximum) (upper resp. lower part of the curves) of the effective potential as function of the $T\sqrt{\lambda}/2$ for several values of the coupling λ

The critical temperature T_c , which is the temperature where the effective potential in its minimum at finite Φ_c equals its value at $\Phi_c = 0$, is in between these two temperatures, closer to T_+ .

The positions of the minimum and the maximum of the effective potential as function of the temperature can be calculated from Eqs. (37) and (36) numerically. Also, they can be taken from (40) except for small values of T where the approximation made in (39) is not valid (there the solution M of Eq. (37) has a nonanalytic behaviour of the type $M \sim_{T \rightarrow 0} \sqrt{2}m + O(\exp(-\frac{\sqrt{2}m}{T}))$). The result is shown in figure 6 for several values of the coupling λ .

It is possible to calculate in a quite easy way the depth of the minimum at $T = T_-$. For this we need the potential at $\Phi_c = 0$ for this temperature. There the gap equation has the (exact) solution $M = 0$. This is just the situation when the curve representing the rhs. in figure 2 starts from zero. Then by means of (57) and (29) we obtain

$$V_{\text{eff}}|_{\Phi_c=0, T=T_-} = -\frac{m^4}{12\lambda} - \frac{\pi^2 T_-^4}{90}.$$

In order to calculate the effective potential in its minimum at $T = T_-$ we use (30) and insert Φ_c from Eq. (36). We obtain

$$V_{\text{eff}}|_{M_{\text{Min}}, T=T_-} = \frac{M_{\text{Min}}^4}{24\lambda} - \frac{m^2 M_{\text{Min}}^2}{6\lambda} - \frac{m^4}{12\lambda} + V_1(M_{\text{Min}}).$$

Now we insert T_- from Eq. (42) and M_{Min} from (40). Expanding V_1 according to (57) we obtain for the difference

$$V_{\text{eff}}|_{M_{\text{Min}}, T=T_-} - V_{\text{eff}}|_{\Phi_c=0, T=T_-} = -\frac{9}{16} \frac{\lambda m^4}{\pi^4}, \quad (43)$$

where higher corrections in λ are dropped. This is the depth of the minimum at the lower spinodal temperature.

It is interesting to calculate the effective mass M in the minima of the effective potential as function of the temperature. This is the so called Debye or temperature dependent mass. For $\Phi_c = 0$ it follows from Eq. (34). At $T = T_+$ we note the value $M_0 = \frac{3}{4}(\sqrt{3}-1)\sqrt{\lambda}m$. In the other minimum it is what we denoted by M_{Min} , given by Eq. (40) (upper sign). At $T = 0$ we note $M_{\text{Min}} = 2m^2$ which is the tree value. At $T = T_-$ we have $M_{\text{Min}} = 3\sqrt{\lambda}m/2\pi$ and at $T = T_+$ we have $M_{\text{Min}} = 3\sqrt{\lambda}m/4\pi$. Both are shown in figure 7 as function of the temperature.

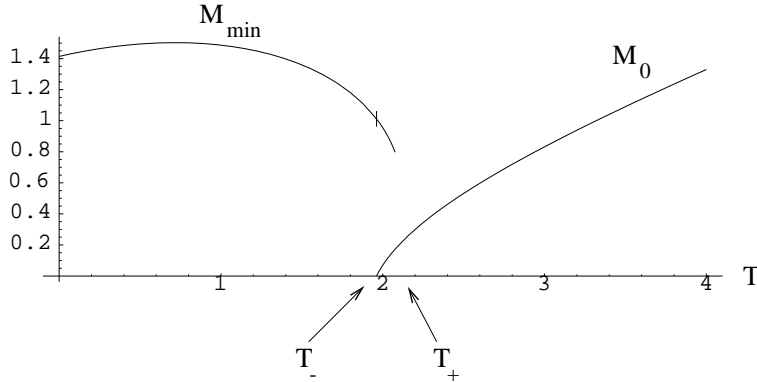


Figure 7: The Debye mass, i.e., the effective mass in the positions of the minima of the effective potential as function of the temperature for $\lambda = 1$

Another important check of the consistency of the given approximation is that in the minimum of the effective potential the term linear in η in the effective action (28) vanishes exactly. This can be seen by inserting Φ_c from (36) and using Eq. (37). Note that from this the disappearance of all tadpole diagrams in the Green functions, not only in the effective action, follows.

Also, the connection between the effective mass and the second derivative of the effective potential in the minimum can be checked. For this reason we calculate $\partial^2 V_{\text{eff}} / \partial(\Phi_c^2)^2$ from (35) and obtain by means of (36) and (37)

$$\frac{\partial^2 V_{\text{eff}}}{\partial(\Phi_c^2)^2} = \frac{1 + 3\lambda\Delta'_0(M)}{1 - 3\lambda\Delta'_0(M)} M^2, \quad (44)$$

with $\Delta' = (\partial\Delta/\partial M^2)$ which is the expected relation within the given approximation.

5 Comparison with different approaches

Since the pioneering papers back to the 70th there have been several steps in the developement of the topic. Already in [4] the necessity of summing 'daisy' and 'super daisy' diagrams was underlined. Perhaps the first summation of 'daisy' diagrams (also called 'ring' diagrams) for different models of quantum field theories was carried out in [19], later on it was reconsidered in [18] with specific application to the electroweak phase transition in the Standard Model. In the latter paper using some high temperature approximations a first order phase transition was obtained where also the imaginary part comes out right. As we will see below, this is a qualitatively good approximation. Detailed information about properties of the high temperature daisy approximation can also be found in [17].

5.1 One Loop Approximation

The simplest approximation is the 'pure $\text{Tr } \ln$ ', which means the one loop contribution to the effective action without summing up any 'daisy' diagrams. The corresponding expression is simply

$$V_{\text{eff}}^a = -\frac{m^2}{2}\Phi_c^2 + \frac{\lambda}{4}\Phi_c^4 + V_1(\mu^2) \quad (45)$$

with $\mu^2 = -m^2 + 3\lambda\Phi_c^2$ and $V_1(m) = \frac{1}{2}\text{Tr } \ln(p^2 + m^2)$. The function V_1 is given in the Appendix, (53), (54). The behaviour of this effective potential is in general well known, but there are some subtles. In order to encounter them we consider the extrema of (45) by equating zero its derivative

$$\frac{\partial V_{\text{eff}}^a}{\partial \Phi_c^2} = -\frac{m^2}{2} + \frac{\lambda}{2}\Phi_c^2 + \frac{3}{2}\lambda\Delta_0(\mu^2), \quad (46)$$

where Eq. (31) had been used. This can be rewritten in the form

$$\mu^2 = 2m^2 - 9\lambda\Delta_0(\mu). \quad (47)$$

This relation is like Eq. (37) with the difference that the effective mass is $\mu^2 = -m^2 + 3\lambda\Phi_c^2$ in this case. In complete analogy to Eq. (37) the solution can be investigated graphically. Figure 5 applies changing merely the coupling according to $\lambda \rightarrow \frac{3}{2}\lambda$. Hence the effective potential has a minimum for $T^2 < 8m^2/3\lambda$. For $T^2 \geq 8m^2/3\lambda$ there are both, a minimum and a maximum. Raising T further they merge and disappear. These are properties of real solutions, i.e., for $\mu^2 > 0$, i.e., $\lambda\Phi_c^2 > m^2/3$. For $\lambda\Phi_c^2 < m^2/3$ the effective potential is complex. Therefore, there might be another minimum if considering only the real part. The effective potential resp. its real and imaginary parts can be easily plotted using formula (54) and the integral representation in (55), see figure 8.

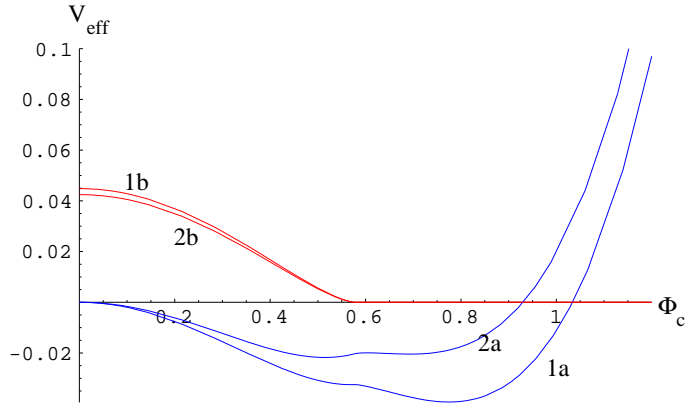


Figure 8: The effective potential in one loop approximation for $\lambda = 1$. Curve 1a resp. 1b shows the real resp. imaginary part for a temperature where the effective potential is real in the lower minimum, curves 2a resp. 2b are for a higher temperature and the effective potential is complex in the lower minimum.

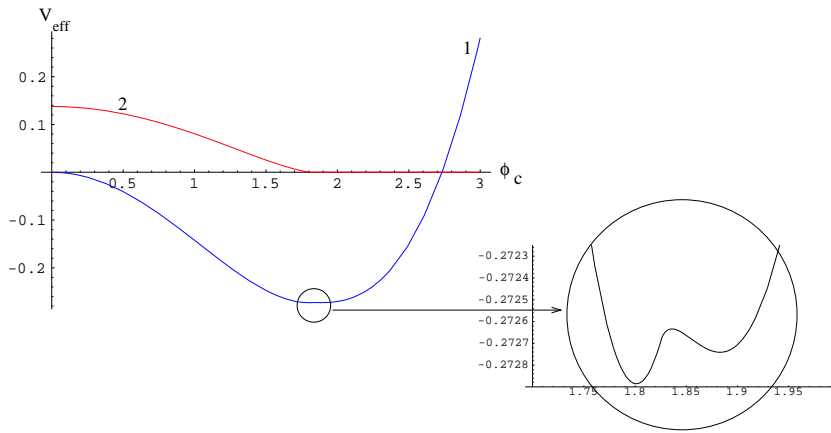


Figure 9: The effective potential in one loop approximation for $\lambda = 0.1$. Curves 1 resp. 2 show the real resp. imaginary part, the magnification shows both minima present.

The general behaviour is that of a second order phase transition. In a narrow temperature region $T^2 \gtrsim 8m^2/3\lambda$ the real part has two minima. At $T^2 < 8m^2/3\lambda$ the left one is lower and for $T^2 > 8m^2/3\lambda$ the right one is the lower one. In the left one the effective potential is complex and in the right one it is real. It seems that the very tiny dip which is shown in figure 8 for $\lambda = 1$ and in figure 9 for $\lambda = 0.1$ in the magnification had not been observed before. It is clear that the pure one loop effective potential is unphysical because it is complex in the minimum at some temperatures. The position of the extrema are shown in figure 11, curves 3,4 and 5 as functions of T . Curve 3 shows the minimum where V_{eff}^a is real, on curve 5 it is complex and curve 4 shows the position of the maximum.

5.2 'Simple Daisy' Diagrams Summed Up

After summing up all 'daisy' and 'super daisy' diagrams, which resulted in the effective potential (29) and the gap equation (27) it is quite simple to go the step back to the simple 'daisy' diagrams summed up by substituting the tree value $\mu^2 = -m^2 + 3\lambda\Phi_c^2$ instead of the effective mass M^2 at two places in these formulae which results in

$$V_{\text{eff}}^b = -\frac{m^2}{2}\Phi_c^2 + \frac{\lambda}{4}\Phi_c^4 - \frac{3}{4}\lambda\Delta_0(\mu) + V_1(M) \quad (48)$$

with

$$M^2 = -m^2 + 3\lambda\Phi_c^2 + 3\lambda\Delta_0(\mu), \quad (49)$$

where V_1 resp. Δ_0 are the same functions (53) resp. (58) as in section 2. However, we have to show that (48) and (49) is just the result of summing the simple 'daisy' diagrams. For this we have to go back to formula (8) and must pick up the daisy diagrams from $W^{1\text{PI}}$. We obtain

$$V_{\text{eff}}^b = -\frac{m^2}{2}\Phi_c^2 + \frac{\lambda}{4}\Phi_c^4 + \frac{1}{2}\text{Tr} \ln(p^2 + m^2) - \frac{1}{8} \text{---} \frac{1}{16} \text{---} \frac{1}{48} \text{---} \dots \quad (50)$$

To be explicit, here we used the notation $\text{Tr} = \frac{1}{\beta} \sum_{l=-\infty}^{\infty} \int \frac{d\vec{k}}{(2\pi)^3}$ and $\text{Tr} \ln(p^2 + m^2) = -\text{Tr} \Delta = -V_1(m)$ where $\Delta = 1/(p^2 + m^2)$ is the line in the graphs (in momentum representation). The vertex factors are -6λ . Now, the analytic expression for the graphs reads

$$\begin{aligned} V_{\text{eff}}^b = & -\frac{m^2}{2}\Phi_c^2 + \frac{\lambda}{4}\Phi_c^4 + \frac{1}{2}\text{Tr} \left[\ln(p^2 + m^2) \right. \\ & \left. - \frac{1}{4} \frac{-6\lambda\Delta_0(m)}{p^2 + m^2} - \frac{1}{8} \frac{(-6\lambda\Delta_0(m))^2}{(p^2 + m^2)^2} - \frac{1}{24} \frac{(-6\lambda\Delta_0(m))^3}{(p^2 + m^2)^3} - \dots \right], \end{aligned} \quad (51)$$

where $\Delta_0(m) = \text{Tr } 1/(p^2 + m^2)$ is in fact the same as (21) resp. (12) written for $T \neq 0$ and with m instead of M . The graph 'eight', 

, can be represented in two ways

$$\text{Diagram} = -6\lambda \left(\text{Tr} \frac{1}{p^2 + m^2} \right)^2 = -6\lambda \text{Tr} \frac{\Delta_0(m)}{p^2 + m^2}$$

(cf. Eq. (12)). Eq. (51) is already the expansion of the logarithm ($\ln(1 + \epsilon) = \epsilon - \epsilon^2/2 + \epsilon^3/3 - \dots$) except for the 'eight', which enters with the wrong sign. In writing the coefficient in front as $\frac{1}{2} = -\frac{1}{2} + 1$ (times 3λ after cancelling a factor of 2) we obtain

$$\begin{aligned} V_{\text{eff}}^b &= -\frac{m^2}{2} \Phi_c^2 + \frac{\lambda}{4} \Phi_c^4 \\ &\quad + \frac{1}{2} \text{Tr} \left[\ln(p^2 + m^2) - \frac{1}{2} \frac{3\lambda\Delta_0(m)}{p^2 + m^2} + \ln \left(1 + \frac{3\lambda\Delta_0(m)}{p^2 + m^2} \right) \right] \\ &= -\frac{m^2}{2} \Phi_c^2 + \frac{\lambda}{4} \Phi_c^4 - \frac{3}{4} \lambda \Delta_0^2(m) + \frac{1}{2} \text{Tr} \ln(p^2 + m^2 + 3\lambda\Delta_0(m)). \end{aligned}$$

This is just (48) and (49).

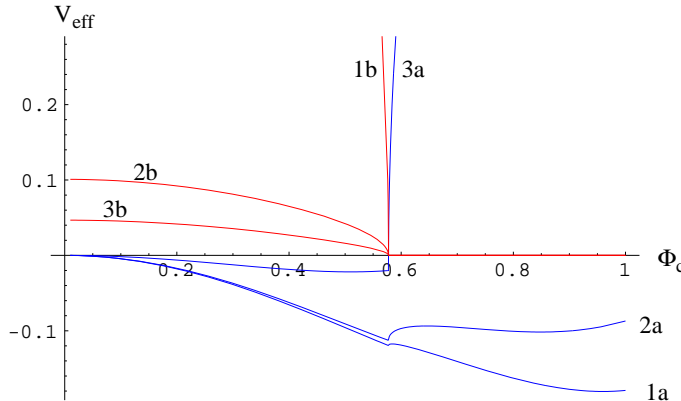


Figure 10: The effective potential with 'simple daisy' graphs summed up for $\lambda = 1$. Curves 1a, 2a, 3a resp. 1b, 2b, 3b show the real resp. imaginary parts for $T = 1, 1, 4, 3.4$.

The investigation of the extrema of V_{eff}^b is more complicated than in the other cases and not very interesting because this case is anyway not physical. Nevertheless it is interesting to comment on them. V_{eff}^b can be plotted quite easily using the above formulae. It is shown in figure 10 as function of Φ_c for several values of the temperature. It has an imaginary part for $\lambda\Phi_c^2 < m^2/3$. At $\lambda\Phi_c^2 = m^2/3$ it has a cusp and above it is real. Again, the real part has two minima in a narrow temperature range. In general, the behaviour is quite similar to that of

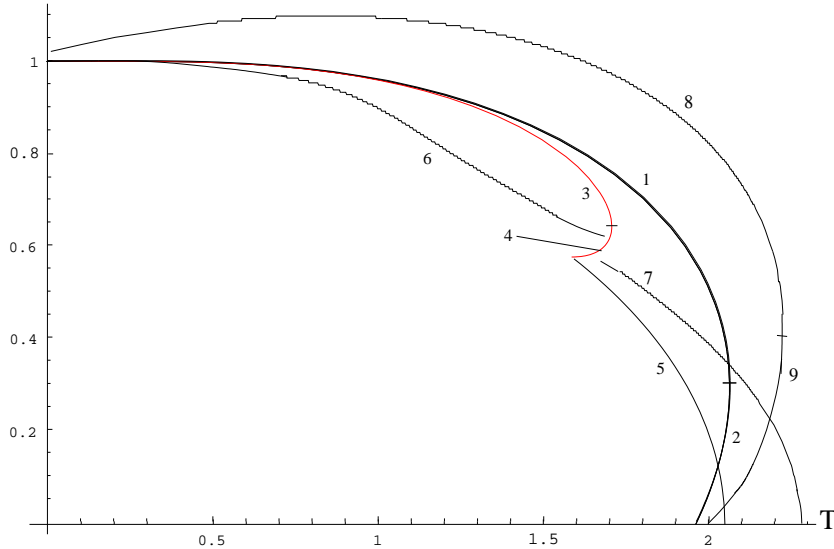


Figure 11: Positions of minima and maxima of the effective potential at $\lambda = 1$ in different approximations, see text

the 'simple Tr ln '. The positions of the minima can be found numerically and they are shown in figure 11 as curves 6 and 7 (the maximum is not shown there). In the minimum represented by curve 7 resp. 6 the effective potential is complex resp. real.

5.3 High Temperature Approximation and higher loop

Frequently high temperature approximations for the functions V_1 and Δ_0 are used which are given by parts of the Eqs. (57), (61). Another type of approximations used can be obtained by taking only the $l = 0$ contribution in the sum over the Matsubara frequencies. A typical example is given in [19]. There, the expression

$$V_{\text{eff}}^t = -\frac{m^2}{2}\Phi_c^2 + \frac{1}{4}\lambda\Phi_c^4 + \frac{T^2}{24}(-m^2 + 3\lambda\Phi_c^2) - \frac{T^2}{12\pi} \left(\frac{\lambda T^2}{4} - m^2 + 3\lambda\Phi_c^2 \right)^{\frac{3}{2}} \quad (52)$$

has been obtained (see also [18]). Here, the phase transition is first order, the effective potential is real in its minima. The positions of the maximum are shown in figure 11 (curve 8 resp. curve 9). It is seen, the behaviour is similar to that of the correct solution (curves 1 and 2), but the numbers are about of 10 ... 20 % higher. So we conclude that the simple formula (52) works basically well and gives a result which is qualitatively correct and quite close to the right numbers.

In the paper [20] the daisy and super daisy graphs have been summed up by direct summation of the graphs performing the difficult task of calculating the combinatorical coefficients (which in the present paper was done implicitly in

section 2). A first order transition resulted. Than the next graph,  , had been included in the resummation. However, the combinatorics could not been done to the end. This is probably the reason that an unwanted imaginary part appeared which led the authors to the conclusion that the subleading terms they calculated are not consistent.

In another paper [21] a similar approach had been undertaken trying to solve the gap equation with two graphs. In a subsequent unpublished paper [27] also, a first order transition was proposed.

6 Conclusions

In the foregoing sections the effective potential for a scalar theory with spontaneous symmetry breaking and finite temperature is calculated. All 'daisy' and 'super daisy' diagrams are summed up and the properties of the resulting gap equation are investigated. It is shown exactly that the phase transition is first order. The imaginary part of the effective action comes out in the correct way.

It is important to notice that higher loop corrections cannot change these features. The point is that they are all expressible in terms of Feynman graphs with propagators $1/(k^2 + M^2)$ (in momentum space) where the mass M is solution of the gap equation. As shown it is positive in the physical region, in the minima of the effective potential for instance (see figure 7). Consequently all graphs have lines with non vanishing denominator. As the theory is Euclidean, no more infrared divergencies can occur. A special discussion deserves the contribution of the graph  . As the vertex factor is $\lambda\Phi_c$ and in the minimum of the effective potential we have $\sqrt{\lambda}\Phi_c \sim 1$ it seems to contribute the same order as the daisy graph. However, this cannot change the conclusion drawn above. It is only the quantitative characteristics of the phase transition which may become altered, not the qualitative ones like its order.

Natural extensions of the present work is the inclusion of fermions, gauge bosons and external fields.

Acknowledgement

VS thanks DFG for support from the grant 436 UKR 17/24/98 and the University of Leipzig for kind hospitality.

Appendix

The function $V_1(M)$ appearing in (29) is the notation for the 'Tr ln' term:

$$V_1(M) = -\frac{1}{2} \text{Tr} \ln \Delta(M) = \frac{1}{\beta} \sum_{l=-\infty}^{\infty} \int \frac{d\vec{k}}{(2\pi)^3} \ln (\omega_l^2 + \vec{k}^2 + M^2) \quad (53)$$

with $\beta = 1/kT$ and $\omega_l = 2\pi l/\beta$. Removing the ultraviolet divergencies and taking into account the normalization conditions the explicit expression reads

$$V_1(M) = \frac{1}{64\pi^2} \left\{ 4m^2 M^2 + M^4 \left[\ln \frac{M^2}{2m^2} - \frac{3}{2} \right] \right\} - \frac{M^2 T^2}{2\pi^2} S_2 \left(\frac{M}{T} \right), \quad (54)$$

where the last term is the temperature dependent contribution. The function S_2 can be represented as a fast converging sum over the modified Bessel function K_2 and by an integral representation which is suited for complex values of the argument as well:

$$S_2(x) = \sum_{n=1}^{\infty} \frac{1}{n^2} K_2(nx) = \frac{1}{3x^2} \int_x^{\infty} dn \frac{(n^2 - x^2)^{3/2}}{e^n - 1}. \quad (55)$$

Its expansion for small x reads

$$S_2(x) = \frac{\pi^4}{45x^2} - \frac{\pi^2}{12} + \frac{\pi x}{6} + \frac{x^2}{32} \left(2\gamma - \frac{3}{2} + 2 \ln \frac{x}{4\pi} \right) + O(x^3), \quad (56)$$

giving rise to the high temperature expansion of V_1 which is at once the expansion for small M :

$$\begin{aligned} V_1(M) &= \frac{-\pi^2 T^4}{90} + \frac{M^2 T^2}{24} - \frac{M^3 T}{12\pi} \\ &+ \frac{1}{64\pi^2} \left\{ M^4 \left[\ln \frac{(4\pi T)^2}{2m^2} - 2\gamma \right] + 4m^2 M^2 \right\} + M^2 T^2 O \left(\frac{M}{T} \right). \end{aligned} \quad (57)$$

Here γ is the Euler constant.

Similar formulae hold for the 'daisy' graph. Although they can be derived by means of (31) it is useful to have them separately:

$$\begin{aligned} \Delta_0(M) &= \frac{1}{\beta} \sum_{l=-\infty}^{\infty} \int \frac{d\vec{k}}{(2\pi)^3} \frac{1}{\omega_l^2 + \vec{k}^2 + M^2} \\ &= \frac{1}{16\pi^2} \left\{ 2m^2 + M^2 \left[\ln \left(\frac{M^2}{2m^2} \right) - 1 \right] \right\} + \frac{MT}{2\pi^2} S_1 \left(\frac{M}{T} \right), \end{aligned} \quad (58)$$

where, again, the last term is the temperature dependent contribution with

$$S_1(x) = \sum_{n=1}^{\infty} \frac{1}{n} K_1(nx) = \frac{1}{x} \int_x^{\infty} dn \frac{\sqrt{n^2 - x^2}}{e^n - 1}. \quad (59)$$

The corresponding expansions are

$$S_1(x) = \frac{\pi^2}{6x} - \frac{\pi}{2} - \frac{x}{8} \left(2\gamma - 1 + 2 \ln \frac{x}{4\pi} \right) + O(x^2) \quad (60)$$

and

$$\Delta_0(M) = \frac{T^2}{12} - \frac{MT}{4\pi} + \frac{1}{16\pi^2} \left\{ M^2 \left(\ln \frac{(4\pi T)^2}{2m^2} - 2\gamma \right) + 2m^2 \right\} + MT O\left(\frac{M}{T}\right). \quad (61)$$

References

- [1] D.A. Kirzhnits. Weinberg model and the 'hot' universe. *JETP Letters*, 15:529–31, 1972. (Pis'ma v Zhurnal Eksperimental'noi i Teoreticheskoi Fiziki, vol.15, no.12, p.745-8 (in Russian)).
- [2] D.A. Kirzhnits and A. Linde. Macroscopic consequences of the weinberg model. *Physics Letters*, 42B:471–4, 1972.
- [3] S. Weinberg. Perturbative calculations of symmetry breaking. *Phys. Rev.*, D7:2887–2910, 1973.
- [4] L. Dolan and R. Jackiw. Symmetry behavior at finite temperature. *Phys. Rev.*, D9:3320–3341, 1974.
- [5] A. Linde. *Particle Physics and Inflationary Cosmology*. harwood academic publishers, 1990.
- [6] J.I. Kapusta. *Finite-temperature field theory*. Cambridge University Press, 1989.
- [7] Jean Zinn-Justin. *Quantum Field Theory and Critical Phenomena*. Clarendon Press, 1996.
- [8] A.H. Васильев. *Квантовополева ренормгруппна в теории критического поведения и стохастической динамике*. Издательство Петербургского института ядерной физики, 1998.
- [9] A. D. Linde. Phase transitions in gauge theories and cosmology. *Rept. Prog. Phys.*, 42:389, 1979.
- [10] David J. Gross, Robert D. Pisarski, and Laurence G. Yaffe. QCD and instantons at finite temperature. *Rev. Mod. Phys.*, 53:43, 1981.
- [11] L. McLerran. The physics of the quark - gluon plasma. *Rev. Mod. Phys.*, 58:1021, 1986.

- [12] O. K. Kalashnikov. QCD at finite temperature. *Fortschr. Phys.*, 32:525–583, 1984.
- [13] Eric Braaten and Robert D. Pisarski. Deducing hard thermal loops from ward identities. *Nucl. Phys.*, B339:310–324, 1990.
- [14] Peter Arnold. The electroweak phase transition: Part 1. review of perturbative methods. 1994. hep-ph/9410294.
- [15] V. A. Rubakov and M. E. Shaposhnikov. Electroweak baryon number non-conservation in the early universe and in high-energy collisions. *Usp. Fiz. Nauk*, 166:493–537, 1996. hep-ph/9603208.
- [16] Vladimir Skalozub and Michael Bordag. Ring diagrams and electroweak phase transition in a magnetic field. 1999. hep-ph/9904333, *Mod. Phys. Lett. A*, to appear.
- [17] M. Dine, R.G, Leigh, P. Huet, A. Linde, and D. Linde. Towards the theory of the electroweak phase transition. *Phys. Rev.*, D46:550, 1992.
- [18] M. E. Carrington. The effective potential at finite temperature in the standard model. *Phys. Rev.*, D45:2933–2944, 1992.
- [19] K. Takahashi. Perturbative calculations at finite temperatures. *Z. Phys.*, C26:601, 1985.
- [20] J. R. Espinosa, M. Quiros, and F. Zwirner. On the phase transition in the scalar theory. *Phys. Lett.*, B291:115–124, 1992.
- [21] Herbert Nachbagauer. On the consistent solution of the gap equation for spontaneously broken lambda ϕ^4 theory. *Z. Phys.*, C67:641–646, 1995.
- [22] N. Tetradis and C. Wetterich. The high temperature phase transition for ϕ^4 theories. *Nucl. Phys.*, B398:659–696, 1993.
- [23] Per Elm fors. Finite temperature renormalization of the ϕ^3 in six- dimensions and ϕ^4 in four-dimensions models at zero momentum. *Z. Phys.*, C56:601–608, 1992.
- [24] A.N. Vasiliev. *Functional Methods in Quantum Field Theory and Statistical Physics*. Gordon and Breach, 1998. (А.Н. Васильев, Функциональные методы в квантовой теории поля и статистике, издательство Ленинградского университета, 1976) (in Russian).
- [25] H.M. Fried. *Basics of Functional Methods and Eikonal Models*. Editions Frontieres, 1990.

- [26] I. T. Drummond, R. R. Horgan, P. V. Landshoff, and A. Rebhan. Foam diagram summation at finite temperature. *Nucl. Phys.*, B524:579, 1998.
- [27] Herbert Nachbagauer. Finite temperature effective potential for spontaneously broken lambda ϕ^4 theory. 1994. hep-ph/9409213.

